Biochemical and Biophysical Research Communications 451 (2014) 196–201

Contents lists available at ScienceDirect

Biochemical and Biophysical Research Communications

journal homepage: www.elsevier.com/locate/ybbrc

Nitroxidative chemistry interferes with fluorescent probe chemistry: Implications for nitric oxide detection using 2,3-diaminonaphthalene

Teh-Min Hu [a,*], Shih-Jiuan Chiu [b], Yu-Ming Hsu [a]

[a] School of Pharmacy, National Defense Medical Center, Taipei, Taiwan, ROC
[b] College of Pharmacy, Taipei Medical University, Taipei, Taiwan, ROC

ARTICLE INFO

Article history:
Received 14 July 2014
Available online 28 July 2014

Keywords:
Nitric oxide
Superoxide
Peroxynitrite
Fluorescent probe
Naphthotriazole

ABSTRACT

Simultaneous production of nitric oxide (NO) and superoxide generates peroxynitrite and causes nitroxidative stress. The fluorometric method for NO detection is based on the formation of a fluorescent product from the reaction of a nonfluorescent probe molecule with NO-derived nitrosating species. Here, we present an example of how nitroxidative chemistry could interact with fluorescent probe chemistry. 2,3-Naphthotriazole (NAT) is the NO-derived fluorescent product of 2,3-diaminonaphthalene (DAN), a commonly used NO-detecting molecule. We show that NO/superoxide cogeneration, and particularly peroxynitrite, mediates the chemical decomposition of NAT. Moreover, the extent of NAT decomposition depends on the relative fluxes of NO and superoxide; the maximum effect being reached at almost equivalent generation rates for both radicals. The rate constant for the reaction of NAT with peroxynitrite was determined to be $2.2 \times 10^3\ M^{-1}\ s^{-1}$. Further, various peroxynitrite scavengers were shown to effectively inhibit NO/superoxide- and peroxynitrite-mediated decomposition of NAT. Taken together, the present study suggests that the interference of a fluorometric NO assay can be originated from the interaction between the final fluorescent product and the formed reactive nitrogen and oxygen species.

1. Introduction

Nitric oxide (NO) is an important, ubiquitous free radical in biological systems. This simple diatomic gas molecule is in no way simple in its chemistry and biological actions. NO mediates various physiological functions via delicately regulated and controlled biosynthetic pathways [1]. Once formed intracellularly, the biotransformation of NO is complicated because of its radical nature [2,3]. On the one hand, NO can immediately react with several metalloproteins and exert its direct biological actions [1]; on the other, NO could react with oxygen and oxidative-stress-derived reactive species, which leads to complex nitroxidative chemistry presumably responsible for the indirect action of NO [1,4,5]. In particular, when NO and superoxide are spatially and temporally coexisting, a potent oxidant, peroxynitrite, is formed instantaneously [5,6]. Under this circumstance, the biological effect of NO is less intuitively predictable because of complex interactions between multiple reactive species and biomolecules [7,8].

A quantitative determination of NO is essential for better understanding the chemistry and biology of NO, but this is not an easy undertaking – given that NO is highly reactive and short-lived. Several methods including electrochemical, chemiluminescent, colorimetric and fluorometric detections have been routinely used for determining the amount of NO generated in both chemical and biological systems [9,10]. Besides its simplicity, sensitivity, and convenience of use, one of the advantages of using a fluorescent compound (probe) to detect NO levels is its potential for allowing continuous real-time measurements [11], although a truly quantitative one remains a challenge. In the case of measuring cellular NO production, a nonfluorescent probe upon cellular uptake would "report" the presence of NO by reacting with NO-derived nitrosating species to form a fluorescent end product [12]. The formation of fluorescent products is a kinetic process involving complex chemistries associated with both nitroxidative species and the probe molecule, which would render it difficult, if not impossible, to conduct a true quantitative determination. Indeed, the fluorescent probes generally do not react directly with NO; they either react with the nitrosating species (e.g., N_2O_3) derived from the autoxidation of NO, or react indirectly with NO via a reactive-nitrogen-species-mediated oxidative process, especially when superoxide or other radicals are also present, that generates free-radical intermediates of the probe molecule [13,14]. The nonspecific nature of the radical intermediates would further react with oxygen or various biomolecules (e.g., antioxidants) to

* Corresponding author. Address: School of Pharmacy, National Defense Medical Center, Taipei 11490, Taiwan, ROC. Fax: +886 2 87923169.
E-mail address: tmhu@ndmctsgh.edu.tw (T.-M. Hu).

http://dx.doi.org/10.1016/j.bbrc.2014.07.097
0006-291X/

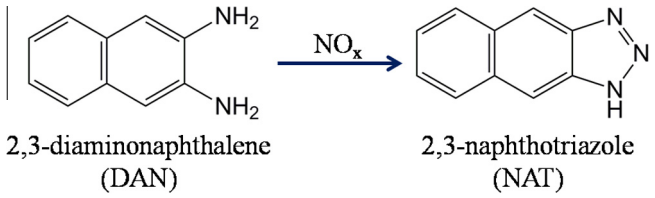

Scheme 1. The rationale of NO detection using 2,3-diaminonaphthalene (DAN). Nonfluorescent DAN reacts with NO-derived nitrosating species (NO_x), forming a fluorescent product (NAT).

produce multiple reactive species that would in turn affect NO levels. While this is a well-recognized, potential problem associated with the use of fluorescent NO probes [12], an issue yet to be addressed is the one linked with the stability of the fluorescent product formed during continuous measurements. This is nontrivial because NO-derived nitroxidative species can be very reactive, possibly making the fluorescent products one of their targets. For example, peroxynitrite, a very reactive molecule produced from NO/superoxide co-generation, is known to react with numerous molecular targets [5,6]. Recently, there have been vigorous pursuits of specific probes for peroxynitrite [15–21]; however, to the best of our knowledge, the reaction of peroxynitrite with the fluorescent product of an NO probe has not been reported.

2,3-Diaminonaphthalene (DAN) has been frequently used in detecting NO levels and nitrosation status in cells and in chemical systems [13,22–26]. The detection is based on the formation of a triazole product (NAT) upon reaction of DAN with reactive nitrogen species (NO_x, Scheme 1, [27,28]). Previously, we unexpectedly observed that SIN-1, a donor of both NO and superoxide, facilitates the fluorescent decay of NAT [29], which prompts us to investigate in detail the putative interaction between the fluorescent probe and the NO/superoxide-derived nitroxidative chemistry. In the present study, we demonstrate that NO/superoxide co-generation mediates the chemical decomposition of NAT. In particular, we show that the extent of NAT decomposition depends on the relative fluxes of NO and superoxide, with a maximum effect occurring at a flux ratio near 1. The result is consistent with the premise that peroxynitrite and its derived reactive species react with NAT, thereby causing its decomposition. Notably, the role of peroxynitrite is confirmed by a kinetic analysis and by experiments in which peroxynitrite scavengers were used.

2. Materials and methods

2.1. Materials

N-[4-[1-(3-aminopropyl)-2-hydroxy-2-nitrosohydrazino]butyl]-1,3-propanediamine (Spermine NONOate; SPENO), 3-morpholinosydnonimine (SIN-1), cytochrome c (horse heart), catalase (bovine liver), glutathione, L-ascorbic acid, uric acid, diethylenetriaminepentaacetic acid (DTPA), and 2,3-diaminonaphthalene (DAN) were obtained from Sigma (St. Louis, MO). 4,4′-[Azobis(oxymethylene]bis-benzoic acid (SOTS-1) and peroxynitrite were purchased from Cayman (Ann Arbor, MI). Potassium phosphate (monobasic) and dimethyl sulfoxide (DMSO) were obtained from J.T. Baker (Phillipsburg, NJ). 2,3-Naphthotriazole (NAT) was synthesized from DAN according to Wheeler et al. [30].

2.2. NAT decomposition kinetics

In the present study, all kinetic experiments were conducted in a fluorometric microplate reader (Infinite M200, Tecan Austria GmbH) with a 96-well microplate format (Nunc, Denmark) at 37 °C. The fluorescence intensity of NAT was measured at excitation and emission wavelengths of 380 and 460 nm (gain = 93), respectively. The reaction buffer consists of 10 mM phosphate buffer (pH 7.4), DTPA (0.1 mM), and catalase (120 U/ml). A typical kinetic run was carried out in a reaction solution (final volume 300 μL) containing 0.5 μM NAT (25 μM stock solution in DMSO), with or without nitroxidative agents. Kinetic runs were initiated by adding various nitroxidative agents alone or in combination to the reaction solution and the fluorescence intensity was followed at 10-min or 5-min intervals up to 120 min. The specific information regarding the preparation of nitroxidative agents in each experimental setup is as follows: (1) the SPENO/SOTS-1 system. The stock solutions for SPENO and SOTS-1 were prepared in 0.01 M NaOH and DMSO, respectively. The final SOTS-1 concentrations in the reaction solution were fixed at 200, 400, 600 μM and the concentrations of SPENO co-added were in the range of 1–200 μM, 60–450 μM, and 60–600 μM, respectively. (2) The peroxynitrite system. An aliquot of 6 μL of diluted peroxynitrite stock solutions (in 0.3 M NaOH) was added to the reaction buffer, giving a final concentration of 50, 100, 200, 300, and 400 μM.

2.3. Estimation of NO fluxes

A spectrophotometric method was used to determine the rate of NO release from SPENO in the reaction system. Specifically, the decomposition kinetics of SPENO (180 μM) in the reaction buffer was determined by measuring the absorbance decrease at 252 nm over time (37 °C) in a UV–visible spectrophotometer (Shimadzu UV-2450, Kyoto, Japan). The first-order rate constant (k_1) for SPENO decomposition was obtained by fitting the kinetic trace. In the present study, the value for k_1 was estimated to be $4.5 \times 10^{-3}\ min^{-1}$. Since the decomposition of 1 mol of SPENO yields 2 mol of NO [31], the rate of NO release at any time t can be estimated from the following equation:

$$\frac{d[NO]}{dt} = 2k_1 \cdot [SPENO]_0 \cdot e^{-k_1 \cdot t} \quad (1)$$

where $[SPENO]_0$ is the initial concentration of SPENO. Thus, the initial NO flux can be calculated from Eq. (2):

$$\frac{d[NO]}{dt} = 2k_1 \cdot [SPENO]_0 \quad (2)$$

2.4. Estimation of superoxide fluxes

The rate of superoxide release from SOTS-1 was determined using a cytochrome c reduction assay. Briefly, cytochrome c was added to the same reaction buffer mentioned above to give a final concentration of 40 μM. To start a kinetic run, SOTS-1 (15–120 μM) was added to the cytochrome c containing buffer. The increase of absorbance at 550 nm as a result of cytochrome c reduction was then followed for 20 min (37 °C). It has been shown that 1 mol of SOTS-1 releases 0.4 mol of superoxide and the process follows first-order kinetics (Eq. (3), [32]):

$$\text{SOTS-1} \xrightarrow{k_2} 0.4O_2^{\cdot-} \quad (3)$$

Eq. (4) shows the reduction of cytochrome c (Fe^{III}cytc) by superoxide; accordingly, the formation of reduced cytochrome c (Fe^{II}cytc) is first-order with respect to superoxide and first-order with respect to oxidized cytochrome c, giving overall a second-order rate expression (Eq. (5)). Under a pseudo-steady-state condition, the rate of cytochrome c reduction is approximately equal to the rate of superoxide production, which is first-order with respect to SOTS-1 (Eq. (5)):

$$O_2^{\cdot-} + Fe^{III}\text{cytc} \xrightarrow{k_3} Fe^{II}\text{cytc} \quad (4)$$

$$\frac{d[Fe^{II}cytc]}{dt} = k_3 \cdot [O_2^{\cdot-}][Fe^{III}cytc] \approx 0.4k_2 \cdot [SOTS\text{-}1] \quad (5)$$

Since [SOTS-1] decreases exponentially with time, Eq. (5) becomes:

$$\frac{d[Fe^{II}cytc]}{dt} = 0.4k_2 \cdot [SOTS\text{-}1]_0 \cdot e^{-k_2 \cdot t} \quad (6)$$

As $t \to 0$, the initial rate of reduction is approximated by Eq. (7), which can be transformed to the expression for the rate of increase in absorbance (A) at 550 nm (Eq. (8)), considering the linear relationship between concentration and absorbance (molar absorptivity, ε):

$$\frac{d[Fe^{II}cytc]}{dt} \approx 0.4k_2 \cdot [SOTS\text{-}1]_0 \quad (7)$$

$$\frac{dA_{550}}{dt} \approx 0.4 \cdot \varepsilon \cdot k_2 \cdot [SOTS\text{-}1]_0 \quad (8)$$

Accordingly, the rate constant for superoxide release (k_2; Eq. (3)) can be estimated from the slope of the plot of the initial velocities of absorbance increases vs. initial concentrations of SOTS-1 (Supplementary Fig. S1). In the present study, the initial velocities were obtained by fitting the initial segments (<10 min) of the kinetic traces. The molar absorptivity ε was taken as 19,600 $cm^{-1}\,M^{-1}$ [33]. The estimated k_2 value is $7.9 \times 10^{-3}\,min^{-1}$. Then, the rate of superoxide formation can be estimated from Eq. (9):

$$\frac{d[O_2^{\cdot-}]}{dt} = 0.4k_2 \cdot [SOTS\text{-}1]_0 \quad (9)$$

2.5. Kinetic analysis for the peroxynitrite–NAT reaction

The reaction between peroxynitrite (PN) and NAT was assumed to follow second-order kinetics. Thus, the rate of PN-mediated changes in NAT concentrations can be expressed as:

$$\frac{d[NAT]}{dt} = -k[PN][NAT] \quad (10)$$

where k is the second-order rate constant. Since in the system the initial concentrations of PN (50–400 μM) is at least 100-fold higher than NAT (0.5 μM) and the spontaneous decay of PN in solution is ultrafast (with a first-order rate constant, k_{PN}, of $0.9\,s^{-1}$ [34,35]), the rate of the change in PN concentrations can be approximately written as:

$$\frac{d[PN]}{dt} = -k_{PN} \cdot [PN] \quad (11)$$

Substituting the solution of Eq. (11), $[PN] = [PN]_0 \cdot e^{-k_{PN} \cdot t}$, into Eq. (10) gives Eq. (12):

$$\frac{d[NAT]}{dt} = -k \cdot [PN]_0 \cdot e^{-k_{PN} \cdot t} \cdot [NAT] \quad (12)$$

which after rearrangement and integration from zero to infinity yields Eq. (13):

$$\ln \frac{[NAT]_{inf}}{[NAT]_0} = -(k/k_{PN}) \cdot [PN]_0 \quad (13)$$

where $[NAT]_{inf}$ is the concentration of NAT at time infinity, and $[NAT]_0$ and $[PN]_0$ are the initial concentrations of NAT and PN, respectively. Because PN would rapidly vanish so that $d[NAT]/dt \to 0$, Eq. (12) implies that as time gets sufficiently large the concentration of NAT would reduce to a remaining steady-state level (i.e. $[NAT]_{inf}$). Thus, Eq. (13) indicates that the fraction of the remaining NAT (i.e. $[NAT]_{inf}/[NAT]_0$) decreases exponentially with the initial concentration of PN, which would give a linear relationship with a slope of $-k/k_{PN}$ in a semilog plot. The second-order rate constant k can then be estimated by knowing k_{PN}. In the present study, the fluorescence intensity (I) of NAT was used to estimate the remaining fraction of NAT, according to the following equations:

$$\ln \frac{[NAT]_{inf}}{[NAT]_0} = \ln \frac{I'_{inf}}{I_0} \quad (14)$$

$$\text{and } I'_{inf} = I_{inf} + \Delta I_{blk} \quad (15)$$

where I'_{inf} is the corrected fluorescence intensity by taking into account the self-quenching effect of NAT; I_{inf} is the measured intensity at 120 min in the presence of PN; ΔI_{blk} represents the change in I at 120 min as a result of the self-quenching effect.

2.6. Effect of peroxynitrite scavengers

SIN-1 or peroxynitrite (100 μM) was added to the reaction buffer containing NAT (0.5 μM) and various concentrations (1–100 μM) of antioxidants (L-ascorbic acid, uric acid, glutathione). The fluorescence intensity (I) of NAT (excitation, 380 nm; emission, 460 nm) was measured at a 10-min interval up to 120 min (37 °C). The inhibitory effect of antioxidants on NAT decomposition was quantified using the following expression:

$$\%\ \text{Inhibition} = 100 \times (I_{antioxidant} - I_{ctl})/(I_{blk} - I_{ctl}) \quad (16)$$

where $I_{antioxidant}$ and I_{ctl} are the measured fluorescence intensity for the experimental and control groups, respectively. I_{blk} is the fluorescence intensity corresponding to the self-quenching effect of NAT.

2.7. HPLC detection of NAT and its reaction product

The experiments were conducted in reaction buffers containing 2 μM NAT and 400 μM SIN-1 or peroxynitrite. A 100 μL aliquot of the reaction solution was taken and injected into HPLC (LC-20AT & SIL-20A, Shimadzu; Mightysil RP-18 GP250-10, 5 μm, Kanto Chemicals, Tokyo, Japan), before and at various times after adding SIN-1 or peroxynitrite. The mobile phase consists of 15 mM phosphate buffer (pH 7.5) and acetonitrile at a ratio of 65/35; the flow rate is 1 mL/min, and the detection is at 369 nm (SPD-20A, Shimadzu, Kyoto, Japan).

3. Results and discussion

3.1. Cogeneration of NO/superoxide mediates NAT decomposition

Previously, we showed that SIN-1, a donor of nitric oxide and superoxide, can facilitate the fluorescence decay of NAT in the reaction buffer. In the present study, we aimed to offer mechanistic insights into the process by using separate donors of nitric oxide and superoxide (i.e. SPENO and SOTS-1, respectively). Specifically, we determined quantitatively the contribution of nitric oxide and superoxide to the decomposition of NAT. Fig. 1A shows that NAT undergoes slight fluorescence bleaching over time, which is not affected by the presence of SOTS-1 or SPENO alone (not shown). However, at a fixed SOTS-1 concentration (600 μM), the kinetic fluorescence traces varied substantially when SPENO was concomitantly added (Fig. 1A). At low SPENO concentrations (up to 120 μM), the traces show an accelerating decline with increasing SPENO concentrations; the effect is generally time-invariant. Remarkably, a transition in the kinetic profile occurs at an intermediate concentration of SPENO (180 μM; the red line): the enhancing effect is attenuated initially (<40 min), whereas it increases at longer reaction times. This biphasic phenomenon (i.e. short-time attenuation and long-time enhancement) becomes much more

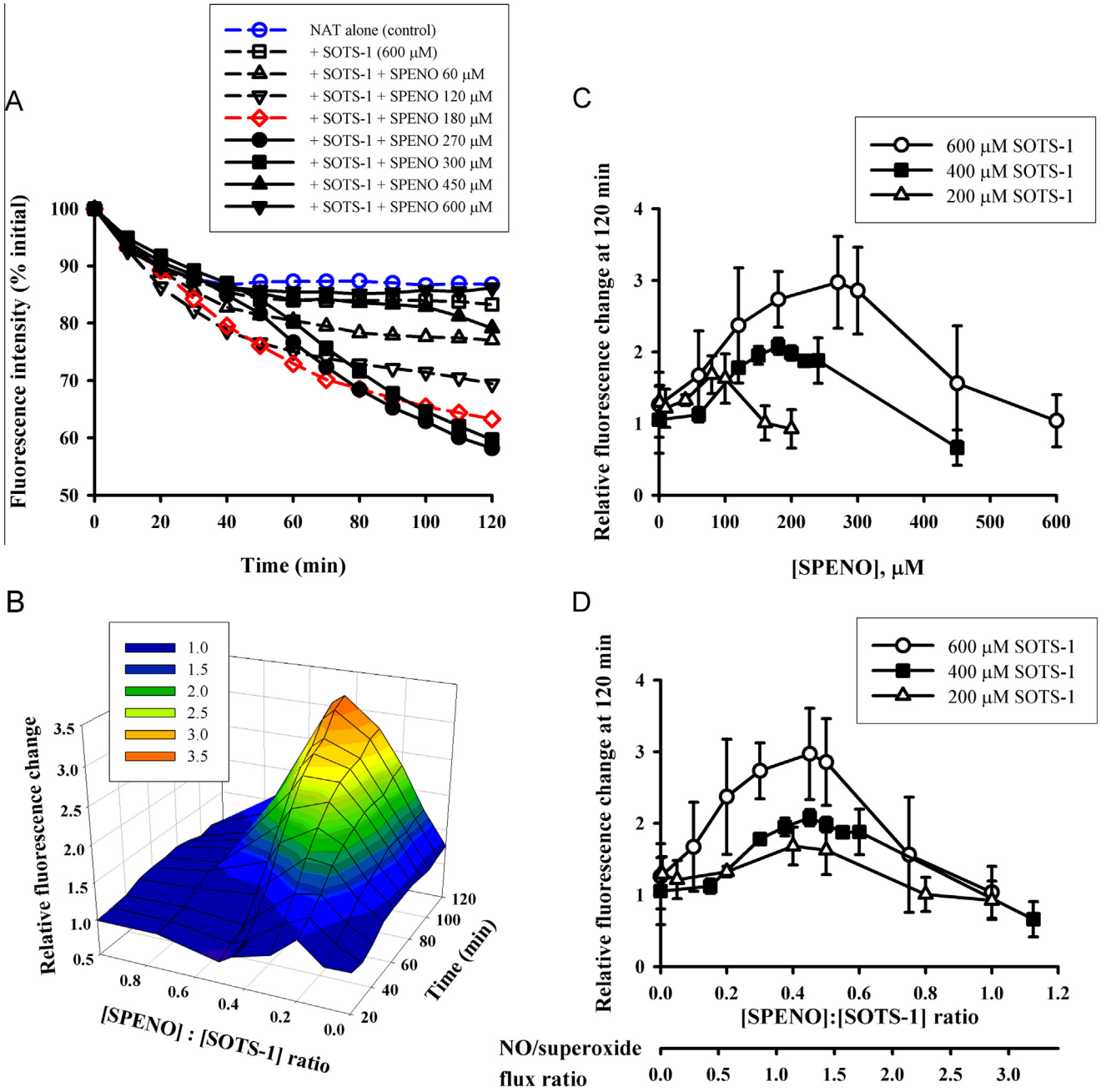

Fig. 1. The coexistence of NO and superoxide donors enhances the fluorescent decay of NAT. (A) Kinetic traces showing the decay of NAT fluorescence over time. Kinetic runs were initiated by adding various concentrations of SPENO (0–600 μM) to the reaction buffer containing 600 μM SOTS-1 and 0.5 μM NAT. (B) Relative fluorescence changes as a function of the donor-concentration ratio and time. The magnitudes of the relative change in fluorescence intensity at different times were calculated from the kinetic traces by normalizing the extent of fluorescence decay (from the initial time to time *t*) for the experimental groups to that for the blank (i.e. NAT alone). (C) Relative fluorescence changes (at 120 min) as a function of SPENO at three fixed levels of SOTS-1 (mean ± SD; n = 3). (D) Relative fluorescence changes as a function of the donor-concentration ratio and the corresponding NO/superoxide flux ratio (mean ± SD; n = 3). (For interpretation of the references to colour in this figure legend, the reader is referred to the web version of this article.)

prominent at [SPENO] = 270–300 μM. At higher concentrations (e.g., ⩾450 μM), however, the enhancement effect is almost completely abolished for the entire reaction period. A 3-D plot shown in Fig. 1B epitomizes the dynamic change of the bell-shaped responses. In particular, it reveals that both the magnitude of the maximum effect and the corresponding optimal donor ratios increase over time. The bell-shaped response can be reproduced at two reduced concentrations of SOTS-1 combined with lower SPENO concentrations (Fig. 1C). It is evident that the maximum response increases with [SOTS-1], along with increases in corresponding [SPENO] – i.e. bigger "bells" with their centers shifting to the right. When the effect was plotted against the molar ratio of SPENO and SOTS-1 (Fig. 1D), all the bell curves, however, aligned vertically with the maximum effect being at the same SPENO/SOTS-1 ratio (~0.5), which corresponds to a nitric oxide/superoxide flux ratio of 1.28.

3.2. Peroxynitrite mediates NAT decomposition

The above findings suggest that the nitroxidative chemistry derived from the coexistence of NO and superoxide plays a significant role in mediating NAT decomposition. Since NO and

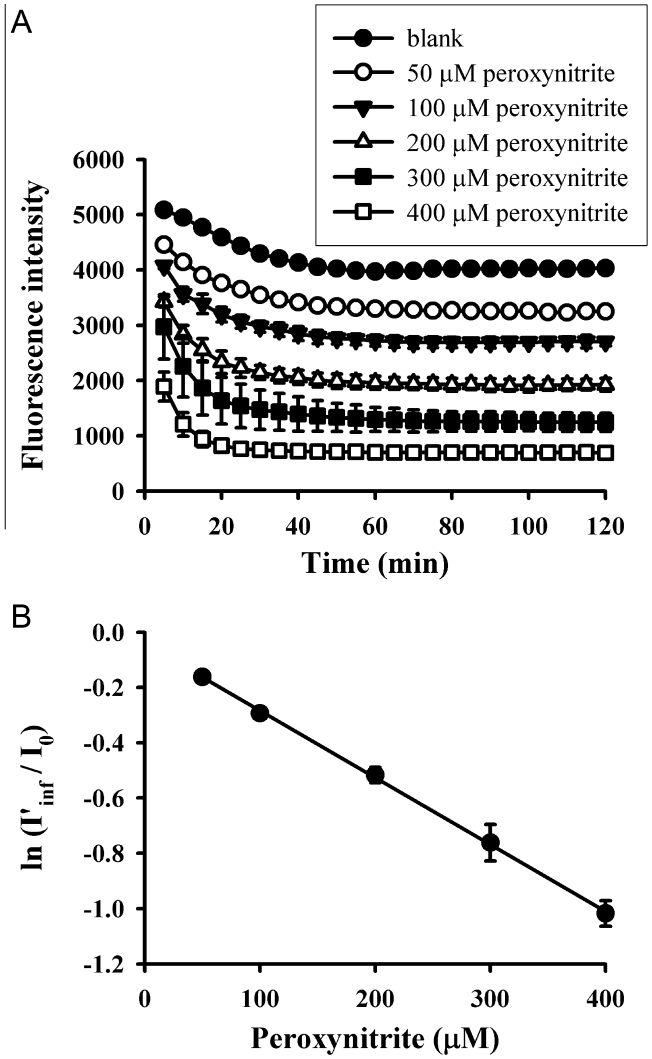

Fig. 2. Peroxynitrite-facilitated fluorescent decay of NAT (mean ± SD; n =3). (A) Kinetic profiles. Kinetic measurements were initiated by adding various concentrations of peroxynitrite (0–400 μM) to the reaction buffer containing 0.5 μM NAT. (B) The relationship between normalized fluorescent changes at 120 min (Eq. (14)) and peroxynitrite concentrations.

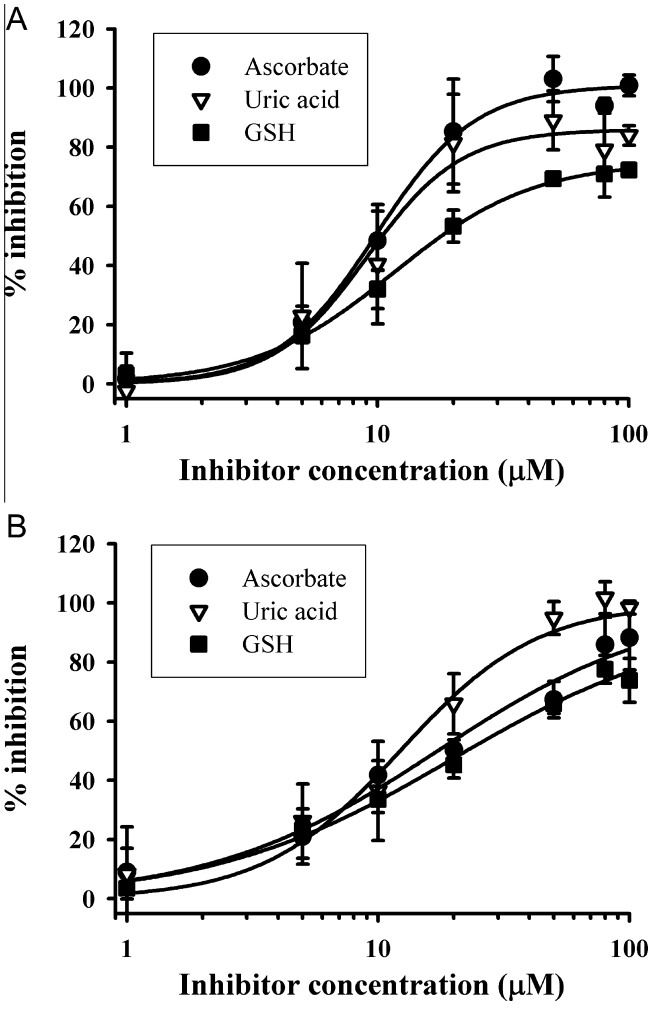

Fig. 3. Peroxynitrite scavengers inhibit SIN-1 and peroxynitrite-mediated NAT decomposition (mean ± SD; n = 3). (A) SIN-1. (B) Peroxynitrite. SIN-1 or peroxynitrite (100 μM) was added to the reaction buffer containing various concentrations (1–100 μM) of antioxidants and NAT (0.5 μM). The fluorescence intensity at 120 min was used to estimate the extent of inhibition (Eq. (16)).

superoxide reacts to form peroxynitrite in a diffusion-limited manner [36], we investigated whether peroxynitrite would exert a destabilizing effect on NAT. The result shown in Fig. 2 indicates clearly that the addition of authentic peroxynitrite causes a rapid concentration-dependent fluorescence decay of NAT. Assuming a second-order reaction between peroxynitrite and NAT, a mathematical expression for the relationship between the remaining amounts of NAT and peroxynitrite concentrations can be deduced (Eq. (13); see Section 2). Accordingly, the fluorescence data shown in Fig. 2A were transformed (based on Eq. (14)) and plotted against [peroxynitrite], which yields an almost perfect linear relationship (Fig. 2B); the fitted slope has a value of $-2420\ M^{-1}$. Since the reported first-order rate constant (k_{PN}) for peroxynitrite decomposition at 37 °C is $0.9\ s^{-1}$ [34,35], the second-order rate constant for the peroxynitrite-NAT reaction is estimated, according to Eq. (16), to be $2.2 \times 10^3\ M^{-1}\ s^{-1}$.

3.3. Effect of peroxynitrite scavengers

To further confirm the role of peroxynitrite in NAT degradation, several biological antioxidants known as peroxynitrite scavengers were added to the reaction buffer containing either SIN-1 or authentic peroxynitrite, and the fluorescence intensity of NAT was then followed over time. The results show that either SIN-1- or peroxynitrite-mediated fluorescence decay was significantly inhibited by the presence of the peroxynitrite scavengers. The degree of inhibition at 120 min was quantified and presented as a function of the inhibitor concentration in Fig. 3. The effects of antioxidants in the two systems are similar, but there are subtle differences. In the SIN-1 system (Fig. 3A), the strongest inhibition was observed for ascorbate, followed by urate and GSH. In the peroxynitrite system (Fig. 3B), urate, however, is the strongest inhibitor. The discrepancy in the findings between the two systems may be due to the possibility that in the SIN-1 system ascorbate can also remove superoxide and nitric oxide [29].

3.4. HPLC analysis of NAT

The reaction mixture was subjected to HPLC analysis to provide chemical evidence for the reaction. The chromatograms recorded after different reaction times (in the SIN-1 system) were shown in Supplementary Fig. S2. It is clear that the peak corresponding to NAT (retention time = 12.4 min) reduces over time. Notably, besides the peaks appearing at 6–7 min that represent the degradation products of SIN-1, a new peak is formed at 3.8 min. Moreover, the same peak was also found in the peroxynitrite system.

Accordingly, the chemical degradation of NAT is evident. Supplementary Fig. S3 shows the quantitative results. As can be seen, the kinetic pattern of the formation of the degradation product coincides well with that of NAT decomposition. It is important to note that the HPLC analysis reproduces the sharp contrast, revealed in the fluorescence study, in kinetics between the SIN-1 and peroxynitrite systems: i.e. slow vs. fast NAT decomposition profiles. This is consistent with the fact the in the SIN-1 system peroxynitrite is formed and its levels are maintained at low sustained levels [29,37], whereas in the peroxynitrite system high bolus peroxynitrite concentrations are given instantaneously.

3.5. Implications for nitric oxide detection using 2,3-diaminonaphthalene (DAN)

DAN has been widely used in the detection of NO and its stable metabolites (nitrite/nitrate) in biological systems. The detection is based on the fluorescent measurement of NAT, which is formed via direct nitrosation or indirect oxidative nitrosylation of DAN [13]. The significance of the present study is that for the first time NAT is shown to be degraded by peroxynitrite, a key reactive species derived from the coexistence of NO/superoxide. Most importantly, our study demonstrates that the extent of NAT degradation varies with the relative fluxes of NO and superoxide, and the dynamically changing effect can be attributed to the formation of peroxynitrite. This could pose an issue for the measurement of biological NO production using DAN. Specifically, our data suggest that the DAN-based determination of NO could be significantly biased in the presence of superoxide and peroxynitrite. The highest bias would occur when NO and superoxide are generated at an approximately equal rate. Moreover, the antioxidant status would also affect the assay result. Thus, the present study serves an important reminder to researchers that caution should be exercised when designing experiments, performing assays, and interpreting data based on the method.

Acknowledgment

The study was supported by Ministry of Science and Technology (MOST) of Taiwan ROC (NSC 102-2320-B-016-003-MY3, NSC 99-2320-B-038-003-MY3).

Appendix A. Supplementary data

Supplementary data associated with this article can be found, in the online version, at http://dx.doi.org/10.1016/j.bbrc.2014.07.097.

References

[1] P. Pacher, J.S. Beckman, L. Liaudet, Nitric oxide and peroxynitrite in health and disease, Physiol. Rev. 87 (2007) 315–424.
[2] R. Radi, Reactions of nitric oxide with metalloproteins, Chem. Res. Toxicol. 9 (1996) 828–835.
[3] B.G. Hill, B.P. Dranka, S.M. Bailey, J.R. Lancaster Jr., V.M. Darley-Usmar, What part of NO don't you understand? Some answers to the cardinal questions in nitric oxide biology, J. Biol. Chem. 285 (2010) 19699–19704.
[4] V. Darley-Usmar, H. Wiseman, B. Halliwell, Nitric oxide and oxygen radicals: a question of balance, FEBS Lett. 369 (1995) 131–135.
[5] G. Ferrer-Sueta, R. Radi, Chemical biology of peroxynitrite: kinetics, diffusion, and radicals, ACS Chem. Biol. 4 (2009) 161–177.
[6] S. Carballal, S. Bartesaghi, R. Radi, Kinetic and mechanistic considerations to assess the biological fate of peroxynitrite, Biochim. Biophys. Acta 2014 (1840) 768–780.
[7] J.R. Lancaster Jr., Nitroxidative, nitrosative, and nitrative stress: kinetic predictions of reactive nitrogen species chemistry under biological conditions, Chem. Res. Toxicol. 19 (2006) 1160–1174.
[8] C.H. Lim, P.C. Dedon, W.M. Deen, Kinetic analysis of intracellular concentrations of reactive nitrogen species, Chem. Res. Toxicol. 21 (2008) 2134–2147.
[9] N.S. Bryan, M.B. Grisham, Methods to detect nitric oxide and its metabolites in biological samples, Free Radic. Biol. Med. 43 (2007) 645–657.
[10] C. Csonka, T. Pali, P. Bencsik, A. Gorbe, P. Ferdinandy, T. Csont, Measurement of nitric oxide in biological samples, Br. J. Pharmacol. http://dx.doi.org/10.1111/bph.12832.
[11] H. Kojima, N. Nakatsubo, K. Kikuchi, S. Kawahara, Y. Kirino, H. Nagoshi, Y. Hirata, T. Nagano, Detection and imaging of nitric oxide with novel fluorescent indicators: diaminofluoresceins, Anal. Chem. 70 (1998) 2446–2453.
[12] P. Wardman, Fluorescent and luminescent probes for measurement of oxidative and nitrosative species in cells and tissues: progress, pitfalls, and prospects, Free Radic. Biol. Med. 43 (2007) 995–1022.
[13] M.G. Espey, D.D. Thomas, K.M. Miranda, D.A. Wink, Focusing of nitric oxide mediated nitrosation and oxidative nitrosylation as a consequence of reaction with superoxide, Proc. Natl. Acad. Sci. USA 99 (2002) 11127–11132.
[14] D. Jourd'heuil, Increased nitric oxide-dependent nitrosylation of 4,5-diaminofluorescein by oxidants: implications for the measurement of intracellular nitric oxide, Free Radic. Biol. Med. 33 (2002) 676–684.
[15] J. Zielonka, A. Sikora, J. Joseph, B. Kalyanaraman, Peroxynitrite is the major species formed from different flux ratios of co-generated nitric oxide and superoxide: direct reaction with boronate-based fluorescent probe, J. Biol. Chem. 285 (2010) 14210–14216.
[16] J. Tian, H. Chen, L. Zhuo, Y. Xie, N. Li, B. Tang, A highly selective, cell-permeable fluorescent nanoprobe for ratiometric detection and imaging of peroxynitrite in living cells, Chemistry 17 (2011) 6626–6634.
[17] F. Yu, P. Song, P. Li, B. Wang, K. Han, A fluorescent probe directly detect peroxynitrite based on boronate oxidation and its applications for fluorescence imaging in living cells, Analyst 137 (2012) 3740–3749.
[18] X. Chen, H. Chen, R. Deng, J. Shen, Pros and cons of current approaches for detecting peroxynitrite and their applications, Biomed. J. 37 (2014) 120–126.
[19] C.C. Winterbourn, The challenges of using fluorescent probes to detect and quantify specific reactive oxygen species in living cells, Biochim. Biophys. Acta 2014 (1840) 730–738.
[20] J. Kim, J. Park, H. Lee, Y. Choi, Y. Kim, A boronate-based fluorescent probe for the selective detection of cellular peroxynitrite, Chem. Commun. (Camb.) (2014), http://dx.doi.org/10.1039/C4CC02943G.
[21] Z.J. Chen, W. Ren, Q.E. Wright, H.W. Ai, Genetically encoded fluorescent probe for the selective detection of peroxynitrite, J. Am. Chem. Soc. 135 (2013) 14940–14943.
[22] A.M. Miles, M.F. Gibson, M. Kirshina, J.C. Cook, R. Pacelli, D. Wink, M.B. Grisham, Effects of superoxide on nitric oxide-dependent N-nitrosation reactions, Free Radic. Res. 23 (1995) 379–390.
[23] M. Fernandez-Cancio, E.M. Fernandez-Vitos, J.J. Centelles, S. Imperial, Sources of interference in the use of 2,3-diaminonaphthalene for the fluorimetric determination of nitric oxide synthase activity in biological samples, Clin. Chim. Acta 312 (2001) 205–212.
[24] D.J. Kleinhenz, X. Fan, J. Rubin, C.M. Hart, Detection of endothelial nitric oxide release with the 2,3-diaminonapthalene assay, Free Radic. Biol. Med. 34 (2003) 856–861.
[25] A. Daiber, S. Schildknecht, J. Muller, J. Kamuf, M.M. Bachschmid, V. Ullrich, Chemical model systems for cellular nitros(yl)ation reactions, Free Radic. Biol. Med. 47 (2009) 458–467.
[26] T.M. Hu, S.C. Ho, Similarity and dissimilarity of thiols as anti-nitrosative agents in the nitric oxide-superoxide system, Biochem. Biophys. Res. Commun. 404 (2011) 785–789.
[27] X.B. Ji, T.C. Hollocher, Mechanism for nitrosation of 2,3-diaminonaphthalene by *Escherichia coli*: enzymatic production of NO followed by O_2-dependent chemical nitrosation, Appl. Environ. Microbiol. 54 (1988) 1791–1794.
[28] A.M. Miles, D.A. Wink, J.C. Cook, M.B. Grisham, Determination of nitric oxide using fluorescence spectroscopy, Methods Enzymol. 268 (1996) 105–120.
[29] T.M. Hu, Y.J. Chen, Nitrosation-modulating effect of ascorbate in a model dynamic system of coexisting nitric oxide and superoxide, Free Radic. Res. 44 (2010) 552–562.
[30] G.L. Wheeler, J. Andrejack, J.H. Wiersma, R.F. Lott, 2,3-Naphthotriazole as a gravimetric, spectrophotometric, and fluormetric reagent for the determination of silver, Anal. Chim. Acta 46 (1969) 239–245.
[31] J.A. Hrabie, J.R. Klose, D.A. Wink, L.K. Keefer, New nitric oxide-releasing zwitterions derived from polyamines, J. Org. Chem. 58 (1993) 1472–1476.
[32] K.U. Ingold, T. Paul, M.J. Young, L. Doiron, Invention of the first azo compound to serve as a superoxide thermal source under physiological conditions: concepts, synthesis, and chemical properties, J. Am. Chem. Soc. 119 (1997) 12364–12365.
[33] V.P. Miller, G.D. DePillis, J.C. Ferrer, A.G. Mauk, P.R. Ortiz de Montellano, Monooxygenase activity of cytochrome c peroxidase, J. Biol. Chem. 267 (1992) 8936–8942.
[34] R. Radi, J.S. Beckman, K.M. Bush, B.A. Freeman, Peroxynitrite oxidation of sulfhydryls. The cytotoxic potential of superoxide and nitric oxide, J. Biol. Chem. 266 (1991) 4244–4250.
[35] W.H. Koppenol, J.J. Moreno, W.A. Pryor, H. Ischiropoulos, J.S. Beckman, Peroxynitrite, a cloaked oxidant formed by nitric oxide and superoxide, Chem. Res. Toxicol. 5 (1992) 834–842.
[36] T. Nauser, W.H. Koppenol, The rate constant of the reaction of superoxide with nitrogen monoxide: approaching the diffusion limit, J. Phys. Chem. A 106 (2002) 4084–4086.
[37] S.C. Ho, S.J. Chiu, T.M. Hu, Comparative kinetics of thiol oxidation in two distinct free-radical generating systems: SIN-1 versus AAPH, Free Radic. Res. 46 (2012) 1190–1200.